ELSEVIER

Journal of Photochemistry and Photobiology A: Chemistry 146 (2001) 19–27

Journal of Photochemistry and Photobiology A:Chemistry

www.elsevier.com/locate/jphotochem

The UV–VIS absorption cross sections of the α-dicarbonyl compounds: pyruvic acid, biacetyl and glyoxal

Abraham Horowitz[1], Richard Meller[2], Geert K. Moortgat*

Division of Atmospheric Chemistry, Max-Planck Institut für Chemie, Postfach 3060, D-55020 Mainz, Germany

Received 10 July 2001; received in revised form 20 September 2001; accepted 2 October 2001

Abstract

The UV–VIS absorption cross sections of the α-dicarbonyl compounds, pyruvic acid and biacetyl (both at 298 K) and of glyoxal (at 295 K), were measured using a diode array detector. In general, the current data for biacetyl and glyoxal are in good agreement with earlier determinations. In the latter case, small deviations from Beer–Lambert law were observed even at pure compound's pressures below 1 Torr. This behavior was not detected in glyoxal–air mixtures at pressures up to 700 Torr. Comparison of the room temperature absorption spectrum of pyruvic acid, determined for the first time in this work, with data obtained at higher temperature reveals that at the lower temperature this spectrum is considerably shifted to the UV. © 2001 Published by Elsevier Science B.V.

Keywords: Pyruvic acid; Biacetyl; Glyoxal

1. Introduction

The dicarbonyl compounds found in the atmosphere are formed by both direct emission and oxidative degradation of hydrocarbons introduced into it from both anthropogenic and biogenic sources. Sources of pyruvic acid ($CH_3COCOOH$) include biomass burning [1], domestic animals [1], plants [2], automotive exhaust [1] and it is a product of atmospheric oxidation of isoprene [3] emitted from trees. Biacetyl ($CH_3COCOCH_3$) and glyoxal (CHOCHO) are important ring cleavage products of the No_x—air photooxidation of aromatic hydrocarbons [4–6]. Photolysis, reaction with hydroxyl radicals and possibly with NO_3 are the main removal channels of these compounds in the troposphere. However, for all three α-carbonyl compounds, photolysis is the major tropospheric loss process [7,8] and thus, the importance of accurate absorption spectral data that serves for the estimation of the atmospheric photodissociation rate constants—*J* values.

Cross sections of the UV–VIS absorption of pyruvic acid have not been measured so far, mainly because of the handling difficulties due to its low vapor pressure and stickiness. However, Yamamoto and Back [9] reported the shape of pyruvic acid's absorption spectrum between 250 and 400 nm at 358 K (in arbitrary units). The absorption spectrum of biacetyl, from 210 to 480 nm, has been reported by Calvert and Pitts [10]. Subsequently, it was also determined by Plum et al. [7] in the wavelength range of 225–480 nm. These authors measured the room temperature cross sections of glyoxal in the same wavelength range as well [7], and their data were reported as a table by Atkinson et al. [11]. Recently, the absorption spectrum of glyoxal has been redetermined at NCAR by Orlando and Tyndall [12].

In view of the importance of direct photolysis as their main atmospheric removal route, the present study of the UV–VIS absorption spectra of the three α-carbonyls: pyruvic acid, biacetyl and glyoxal has been undertaken in order to obtain the yet unavailable data for the first one and to verify the data for the other two of these compounds.

2. Experimental

2.1. Materials

Biacetyl (Fluka, stated purity > 99%) was used as received. Pyruvic acid (Aldrich, stated purity 98%) was purified by trap to trap distillation, retaining the middle fraction which, unlike the slightly yellowish originally supplied material, was colorless. FT-IR spectral analyses of the

* Corresponding author.
E-mail address: moo@mpch-mainz.mpg.de (G.K. Moortgat).
[1] Co-corresponding author. Permanent address: Soreq NRC, Yavne 81800, Israel.
[2] Present address: 16 Evergreen Lane, Manhattan Beach, CA 90266, USA.

1010-6030/01/$ – see front matter © 2001 Published by Elsevier Science B.V.
PII: S1010-6030(01)00601-3

distilled pyruvic acid did not reveal presence of impurities. Glyoxal was prepared by decomposing its trimer hydrate at 150–160 °C in the presence of P_2O_5 and under N_2 flow. It was collected as yellow crystals at dry ice–ethanol temperature and was stored at −16 °C. As indicated by the amount of impurities detected in the FT-IR spectra, this procedure yields glyoxal with a purity better than 99%. Nevertheless, as an additional precaution, prior to the determination of glyoxal's absorption spectrum it was further purified by trap to trap distillation and from the retained middle fraction the first 0.5 Torr were always pumped out. Mixtures of glyoxal with synthetic air were prepared in 6 l bulb. In order to ensure complete mixing, these mixtures were left to stand for at least 3 h prior to the spectral measurements. Loss of glyoxal was not observed in these mixtures even after 24 h of standing.

2.2. Apparatus and procedures

The experimental set-up used in the present work was similar to that employed in earlier studies in which the absorption spectra of methylglyoxal [13] and $CF_3C(O)Cl$ [14] were determined. Absorbances of the gases and gaseous mixtures, introduced from a grease-free vacuum line at a pressure measured by a Baratron capacitances pressure gauges (MKS, 10 and 1000 Torr range), were determined in a 30 mm i.d. cell with suprasil windows. The temperature in the cell was maintained constant (±0.2 K) by circulating a thermostated liquid through a glass cylinder surrounding it. For the biacetyl experiments, the optical length was 63 cm. In the case of pure glyoxal and in particular, in the case of pyruvic acid, problems due to condensation and polymerization at the walls of the cell were encountered and their effect was reduced by using a cell with an extended path of 106 cm and heating of the windows to about 60 °C.

A 200 W deuterium lamp (Heraeus) and a 60 W tungsten/halogen lamp were used as light sources. To prevent detection of stray light and light coming from higher order reflections from the grating, various filters were introduced into the beam before it entered the cell. After transversing the cell, the beam was collimated on the entrance slit of the 0.6 m Czerny–Turner type monochromator (Jobin–Yvon) where it was dispersed by a 600 groves/mm grating and then refocused on a 1024 pixel photo-diode array (PDA) connected to a PC that served for data storage and processing. Under these conditions, 70 nm windows were obtained at each monochromator setting with a nominal resolution of 0.07 nm/pixel and effective resolution of (spectral full width at half trace height-bandpath) of ∼0.25 nm, as determined for the Hg lines from the penray lamp that was used for calibration. The typical overlap between adjacent windows was 20 nm (e.g. 10 nm at each end).

Absorption cross sections (σ (cm^2 per molecule)) at a given wavelength (λ (nm)) were derived from the Beer–Lambert's law.

$$\sigma(\lambda) = \frac{\ln[I_0(\lambda)/I(\lambda)]}{lC} \quad (1)$$

where l is the optical path length (cm), C the concentration (molecule cm^{-3}) and $I_0(\lambda)$ and $I(\lambda)$ represent

Table 1
Absorption cross sections (cm^2 per molecule) of pyruvic acid at 298 K (averaged over 1 nm intervals)

λ (nm)	$10^{20}\sigma$	λ (nm)	$10^{20}\sigma$	λ (nm)	$10^{20}\sigma$
252	1.544	304	0.687	356	3.432
253	1.546	305	0.756	357	3.227
254	1.607	306	0.824	358	3.034
255	1.556	307	0.894	359	2.847
256	1.521	308	0.969	360	3.068
257	1.409	309	1.032	361	3.197
258	1.246	310	1.095	362	2.990
259	1.071	311	1.161	363	2.638
260	0.908	312	1.214	364	2.516
261	0.801	313	1.269	365	2.575
262	0.737	314	1.335	366	2.451
263	0.718	315	1.416	367	2.570
264	0.718	316	1.543	368	2.746
265	0.700	317	1.685	369	3.087
266	0.651	318	1.780	370	2.835
267	0.566	319	1.906	371	2.521
268	0.470	320	2.043	372	1.766
269	0.367	321	2.136	373	1.510
270	0.278	322	2.233	374	1.453
271	0.224	323	2.294	375	1.065
272	0.195	324	2.332	376	0.910
273	0.185	325	2.408	377	0.820
274	0.182	326	2.510	378	0.702
275	0.188	327	2.556	379	0.504
276	0.189	328	2.612	380	0.336
277	0.180	329	2.744	381	0.241
278	0.164	330	2.893	382	0.179
279	0.139	331	3.051	383	0.146
280	0.118	332	3.312	384	0.122
281	0.101	333	3.512	385	0.097
282	0.093	334	3.515	386	0.084
283	0.098	335	3.563	387	0.077
284	0.104	336	3.610	388	0.066
285	0.113	337	3.602	389	0.056
286	0.124	338	3.584	390	0.047
287	0.138	339	3.542	391	0.034
288	0.156	340	3.475	392	0.031
289	0.173	341	3.500	393	0.026
290	0.190	342	3.714	394	0.015
291	0.210	343	3.753	395	0.011
292	0.234	344	3.729	396	0.006
293	0.258	345	3.766	397	0.002
294	0.289	346	4.019	398	0.002
295	0.322	347	4.089	399	$<1 \times 10^{-23}$
296	0.352	348	4.243		
297	0.386	349	4.412		
298	0.421	350	4.473		
299	0.456	351	4.268		
300	0.490	352	4.118		
301	0.529	353	4.056		
302	0.578	354	3.968		
303	0.633	355	3.648		

the light intensities of the light transmitted by the evacuated and filled cell, respectively. The applicability of Eq. (1) was examined by measuring the variation of absorbance with the pressure of the absorbing gas in the cell and it was verified for biacetyl and pyruvic acid. In the case of pure glyoxal, deviations from this law were observed for the pure compound (see in the following sections). The final cross sections reported here are based on the average values derived from six to ten separate measurements.

3. Results and discussion

3.1. Pyruvic acid

Pyruvic acid has a relatively low pressure at room temperature of about 1.2 Torr. Consequently, as indicated by the pressure drop in the cell, it condensed on its walls even when introduced at the minimum pressures necessary for a meaningful quantitative measurement of its absorbance in the 106 cm long cell used by us. The heating of the windows reduced their coating and the resultant scatter of the data. Further improvement of the reproducibility was achieved by adopting a procedure according to which the cell was first conditioned by exposing it for 5 min to the acid at the pressure at which the absorbance was to be measured. Subsequently, the cell was evacuated until the pressure reached $\sim 1 \times 10^{-3}$ Torr, i.e. without waiting until the acid that accumulated on the walls was completely pumped out. At this stage, the cell was closed and the measured intensity of the transmitted light was taken as equal to I_0. The acid was then introduced into the cell and the spectrum of each sample was recorded twice. The pressure in the cell was continuously monitored during the recording of the spectra. The pressure drop decreased with time, amounting to about 5% during the first measurement and it was less than 2% during the second one. In the calculation of the cross sections, the average pressure during each of the measurements were used and the values thus derived were in good agreement. Application of this procedure allowed measurements in the pressure range of 0.2–0.8 Torr in which the applicability of Beer–Lambert's law was verified. However, in these measurements the results at the lower end of the pressure range were considerably more scattered than those at the high pressure end and therefore, the final measurements, on which the absorption cross section reported here are based, were all conducted at pressures between 0.7 and 0.8 Torr.

The 298 K absorption cross sections of pyruvic acid averaged over 1 nm intervals are listed in Table 1 while a plot of the original data is shown in Fig. 1. The cross section at the absorbance peak at 350.12 nm was found to be $(4.51 \pm 0.11) \times 10^{-20}$ cm^2 per molecule where the error limits equal two standard deviations (2σ). However,

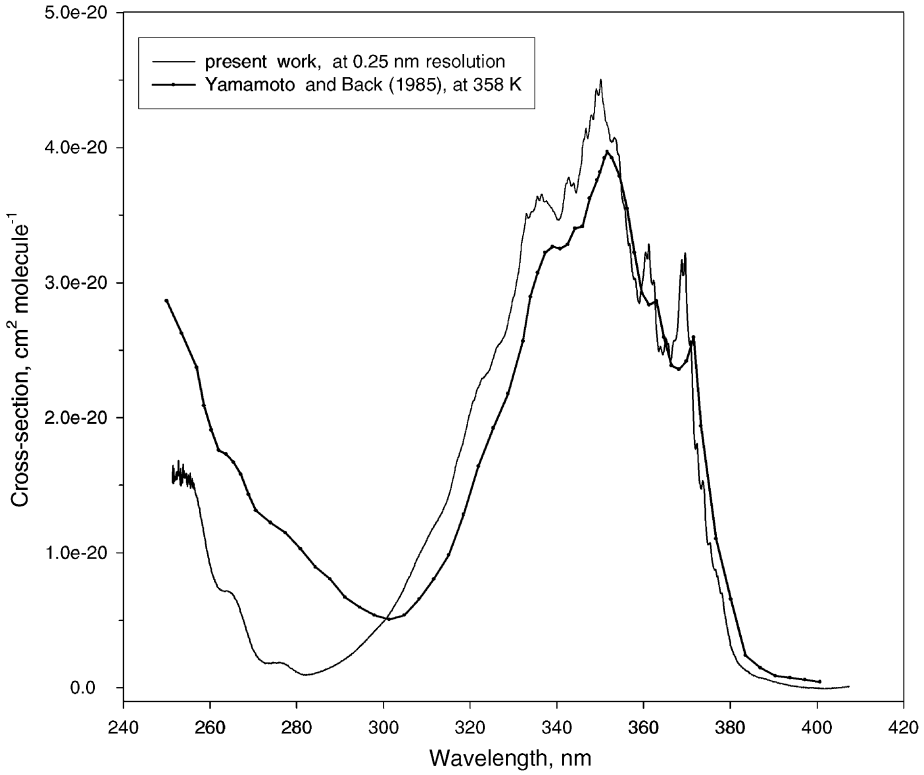

Fig. 1. The UV–VIS absorption spectrum of pyruvic acid: a comparison of the present results with those of Yamamoto and Back [9] according to Ref. [15], see text.

examination of the potential sources of error in our measurements and taking into account the possibility of dimer presence (see the following paragraphs), leads to a more realistic estimated accuracy of ±12% and not less than 2.0×10^{-21} cm^2 per molecule.

The absorption spectrum of pyruvic acid was also determined by Yamamoto and Back [9] whose measurements were carried out in a 4 m long cell held at 85 °C and a pressure of 4.85 Torr. The original work reports only the relative absorbances at the above pressure. Nevertheless, absolute

Table 2
Absorption cross sections (cm^2 per molecule) of biacetyl at 298 K (averaged over 1 nm intervals)

λ (nm)	$10^{20}\sigma$	λ (nm)	$10^{20}\sigma$	λ (nm)	$10^{20}\sigma$	λ (nm)	$10^{20}\sigma$	λ (nm)	$10^{20}\sigma$	λ (nm)	$10^{20}\sigma$
206	10.30	260	4.270	314	0.480	368	1.660	422	7.250	476	0.031
207	9.860	261	4.410	315	0.438	369	1.760	423	7.240	477	0.028
208	9.140	262	4.460	316	0.405	370	1.850	424	7.130	478	0.025
209	7.970	263	4.490	317	0.380	371	1.940	425	6.980	479	0.023
210	6.740	264	4.490	318	0.360	372	2.020	426	6.810	480	0.021
211	5.820	265	4.480	319	0.344	373	2.100	427	6.570	481	0.019
212	5.180	266	4.490	320	0.334	374	2.170	428	6.430	482	0.018
213	4.700	267	4.540	321	0.331	375	2.250	429	6.340	483	0.017
214	4.290	268	4.630	322	0.321	376	2.330	430	6.310	484	0.016
215	3.900	269	4.810	323	0.295	377	2.410	431	6.400	485	0.015
216	3.550	270	4.950	324	0.261	378	2.500	432	6.630	486	0.015
217	3.210	271	5.000	325	0.232	379	2.580	433	6.780	487	0.015
218	2.900	272	4.980	326	0.212	380	2.680	434	6.780	488	0.015
219	2.580	273	4.920	327	0.200	381	2.790	435	6.720	489	0.016
220	2.260	274	4.850	328	0.194	382	2.920	436	6.560	490	0.018
221	1.960	275	4.760	329	0.193	383	3.070	437	6.400	491	0.019
222	1.700	276	4.700	330	0.196	384	3.220	438	6.420	492	0.021
223	1.500	277	4.680	331	0.203	385	3.390	439	6.280		
224	1.350	278	4.670	332	0.212	386	3.530	440	6.510		
225	1.270	279	4.680	333	0.199	387	3.670	441	6.670		
226	1.230	280	4.710	334	0.216	388	3.820	442	6.990		
227	1.240	281	4.730	335	0.231	389	4.000	443	7.230		
228	1.280	282	4.650	336	0.245	390	4.170	444	6.850		
229	1.340	283	4.500	337	0.263	391	4.340	445	6.490		
230	1.410	284	4.320	338	0.284	392	4.470	446	5.900		
231	1.470	285	4.140	339	0.296	393	4.560	447	5.430		
232	1.530	286	3.940	340	0.298	394	4.620	448	5.010		
233	1.590	287	3.770	341	0.318	395	4.670	449	4.330		
234	1.680	288	3.620	342	0.346	396	4.730	450	4.060		
235	1.800	289	3.500	343	0.365	397	4.820	451	3.440		
236	1.920	290	3.380	344	0.387	398	4.920	452	3.200		
237	2.090	291	3.280	345	0.412	399	5.020	453	2.650		
238	2.150	292	3.200	346	0.442	400	5.120	454	2.160		
239	2.210	293	3.110	347	0.469	401	5.190	455	1.720		
240	2.290	294	2.960	348	0.499	402	5.260	456	1.390		
241	2.390	295	2.730	349	0.534	403	5.380	457	1.140		
242	2.540	296	2.500	350	0.565	404	5.540	458	0.853		
243	2.690	297	2.290	351	0.607	405	5.750	459	0.726		
244	2.800	298	2.100	352	0.650	406	6.000	460	0.549		
245	2.890	299	1.930	353	0.683	407	6.260	461	0.454		
246	2.940	300	1.770	354	0.729	408	6.470	462	0.356		
247	2.990	301	1.640	355	0.771	409	6.590	463	0.280		
248	3.050	302	1.540	356	0.815	410	6.690	464	0.219		
249	3.150	303	1.460	357	0.864	411	6.820	465	0.179		
250	3.310	304	1.380	358	0.916	412	6.970	466	0.143		
251	3.480	305	1.320	359	0.966	413	7.110	467	0.118		
252	3.600	306	1.270	360	1.020	414	7.310	468	0.096		
253	3.680	307	1.210	361	1.080	415	7.470	469	0.081		
254	3.730	308	1.100	362	1.190	416	7.570	470	0.069		
255	3.750	309	0.950	363	1.260	417	7.620	471	0.059		
256	3.780	310	0.815	364	1.330	418	7.510	472	0.051		
257	3.840	311	0.707	365	1.410	419	7.390	473	0.044		
258	3.940	312	0.616	366	1.490	420	7.370	474	0.040		
259	4.090	313	0.539	367	1.570	421	7.320	475	0.035		

values can be derived from their results using the value $\sigma = 3.82 \times 10^{-20}$ cm^2 per molecule at 350 nm quoted by Berges and Warneck [15]. The normalized spectrum thus obtained is shown in Fig. 1. Although the general shape of the spectrum derived in this manner is quite similar to the one determined in the present work, it is quite evident that the spectrum obtained by Yamamoto and Back is shifted to the red. In addition, below about 300 nm their cross section are considerably higher. Conceivably, at least in part, these differences can be ascribed to the effect of temperature, whereby lowering of temperature is accompanied by association of the pyruvic acid molecules in analogy with similar behavior of carboxylic acids. However, since deviations from the linear dependence predicted by Beer–Lambert's law were not observed, this does not seem to be the case, unless practically all of the pyruvic acid was present as a dimer. At the low pressures used, this appears to be a rather unlikely situation. Furthermore, suppose that sizable amounts of a dimer were formed at the pressures employed and that the expected significant curvature of the Beer–Lambert's plot was undetected because of the previously mentioned scatter in the lower pressure absorbances. In this case, the shape of the absorption spectrum should change with pressure. Such a change was not observed and hence, we conclude that only a small amount of the pyruvic acid, which in order to be on the safe side we estimate as $<$10%, might have been present as a dimer.

3.2. Biacetyl

The absorption cross sections of biacetyl were measured in the pressure range of 0.5–10 Torr in which deviations from Beer–Lambert's law were not observed. In Table 2, cross sections averaged over 1 nm intervals are listed. For cross section longer than $\sim 2 \times 10^{-20}$ cm^2 per molecule, the scatter of the data, as represented by standard deviations of the average values, did not exceed 2% (2σ). However, taking into account the potential errors due to instrumental inaccuracies, we estimate that the accuracy of the biacetyl data derived in this work as being $\pm$4% and not less than $\pm 1 \times 10^{-21}$ cm^2 per molecule (the highest of the two).

The original (unaveraged) spectrum is shown in Fig. 2 together with the spectrum determined by Plum et al. [7], and Atkinson et al. [11] as well as the one reported by Calvert and Pitts [10]. It can be seen that the agreement between the values derived in the present work and those obtained in the other two studies is quite good.

3.3. Glyoxal

Similarly to biacetyl, glyoxal has two absorption bands in the region above 220 nm, one in the UV and the other in the visible. The UV absorbance of pure glyoxal in the pressure range 0.2–10 Torr followed the expected linear pressure

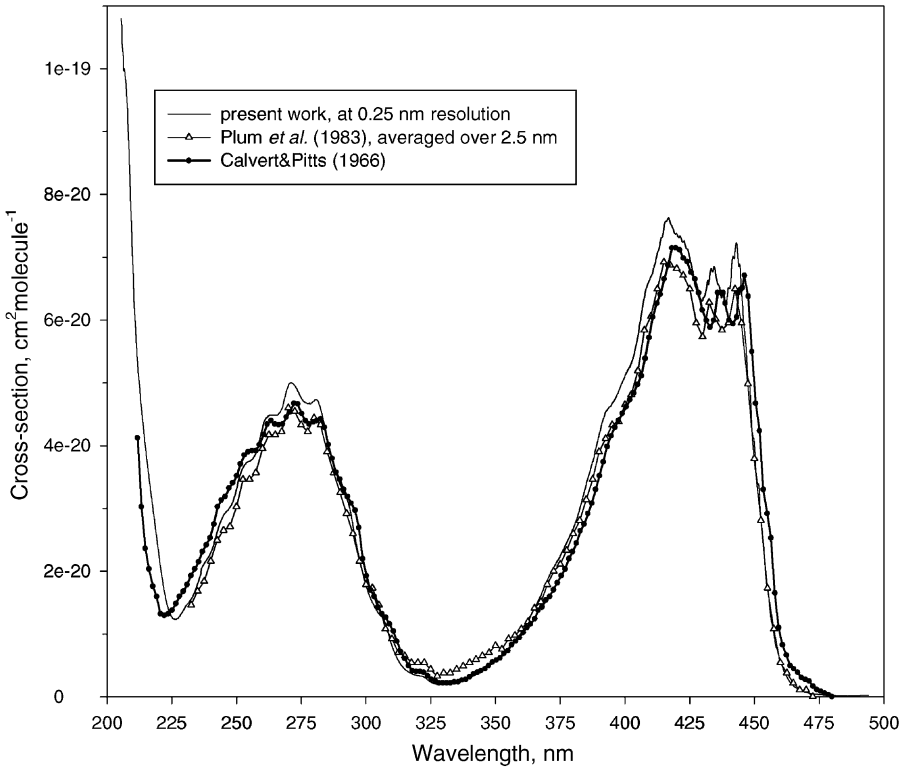

Fig. 2. The UV–VIS absorption spectrum of biacetyl: a comparison of the present results with those of Calvert and Pitts [10] and of Plum et al. [7].

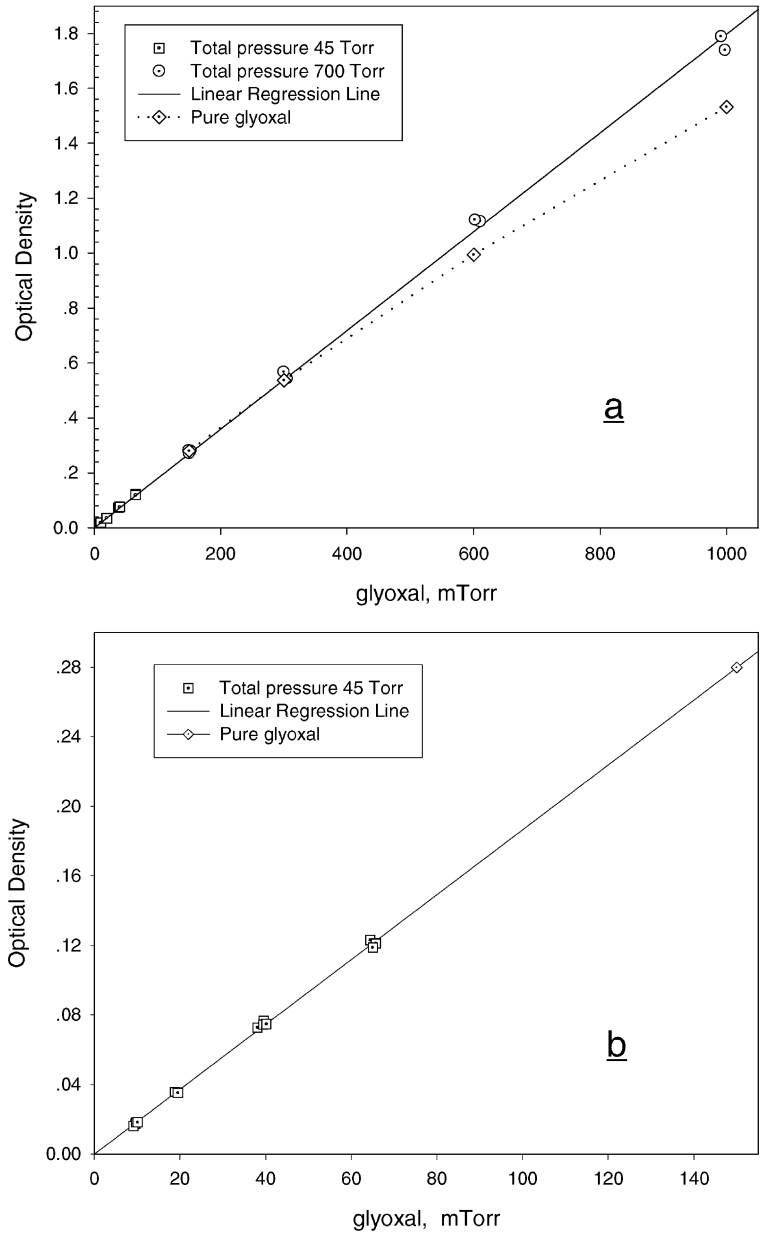

Fig. 3. Beer–Lambert's plot of optical density at 455.30 nm vs. glyoxal's pressure in both pure glyoxal and its mixtures with air: (a) p(glyoxal): 0–1.0 Torr; (b) p(glyoxal): 0–0.15 Torr (expanded low pressure range).

dependence. However, in the visible band, where the spectrum is more structured and the absorption cross sections are higher, deviation from Beer–Lambert's law was observed even at pressures above 0.3 Torr. We have studied this effect in detail, in both pure glyoxal and its mixtures with synthetic air, at pressures from 45 to 700 Torr. The observed typical behavior of the absorbance at the peak at $\lambda = 455.30$ nm, where the deviation from linearity was most pronounced, is shown in Fig. 3. As can be seen from Fig. 3a, in glyoxal–air mixtures up to the partial pressure of 1 Torr of glyoxal, the plot of optical density versus glyoxal pressure is linear over the entire total range of air pressures. On the other hand, at this pressure of pure glyoxal (1 Torr) a significant departure (∼15%) from the expected line can be seen. As shown in Fig. 3a and in more detail in Fig. 3b, at about 0.3 down to 0.01 Torr, Beer–Lambert's law is obeyed both in air mixtures of glyoxal and in the pure samples and the individual curves converge to a single straight line.

Although the above described observations do not provide a clue as to the origin of the deviations from linearity, they clearly indicate that this effect must be a consequence of some experimental artifact that has an insignificant effect on the absorbance of glyoxal at the peak at pressures below 0.3 Torr. Experimentally we have seen that for other

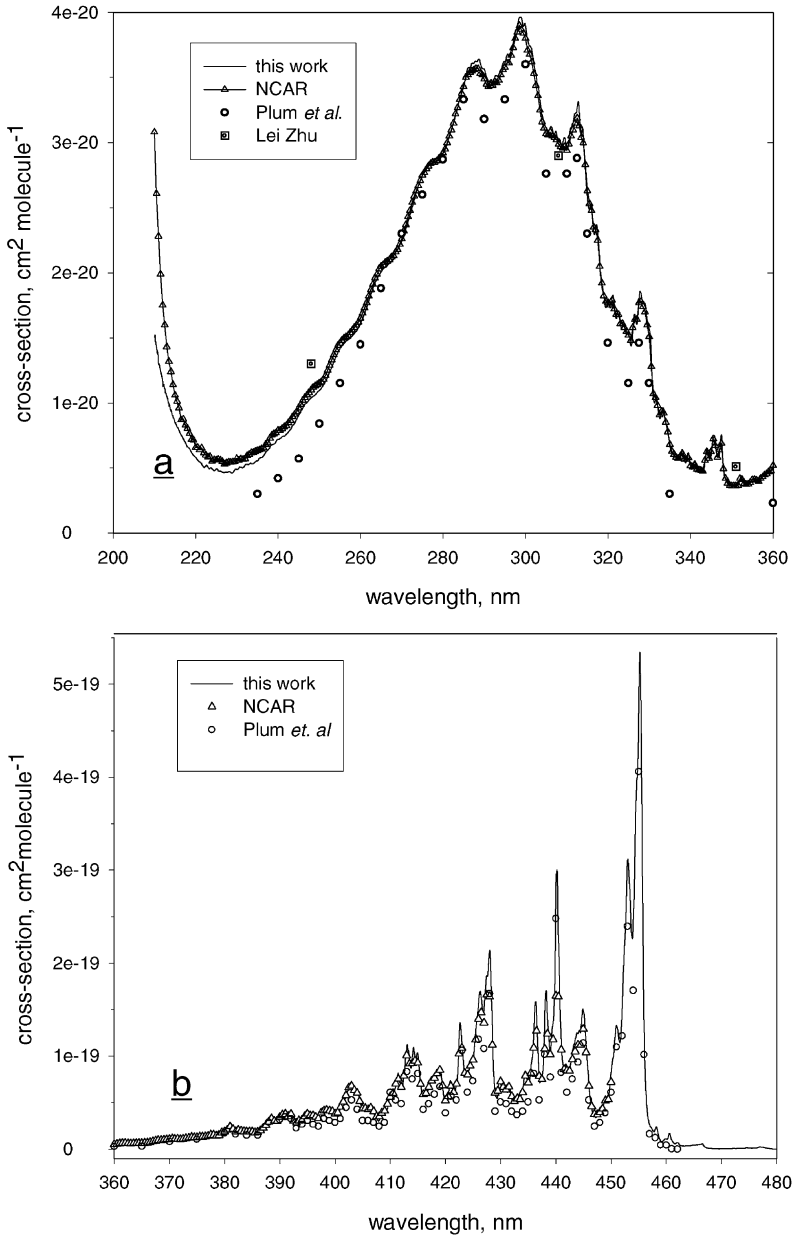

Fig. 4. The UV–VIS absorption spectrum of glyoxal: a comparison of the present results with those of Plum et al. [7], NCAR [12] and Zhu et al. [16]; (a) the UV region and (b) the visible region.

wavelengths in this band, the lower the measured cross section was, the range in which linearity was observed extended to much higher pressures.

Based on these results, we have determined the absorption spectrum of glyoxal presented in Fig. 4 from which the 1 nm averaged cross sections listed in Table 3 were derived. Although for cross sections higher than 2×10^{-20} cm^2 per molecule the observed scatter (2σ) did not exceed 1.5%, a more realistic assessment of our results and of potential sources of error leads to an estimated accuracy of $\pm 5\%$ but not less than $\pm 1.5 \times 10^{-21}$ cm^2 per molecule.

In Fig. 4, the present results are compared with the cross sections derived in several other studies. It can be seen (see Fig. 4a) that the few measurements of Zhu et al. [16] yield cross sections that seem to lie on the curve determined by our results. Except for the region in which $\lambda < 240$ nm, throughout almost the entire wavelength range, the results of Orlando and Tyndall (NCAR) are in very good agreement with the present values. The agreement between our results and those of Plum et al. [7] is also quite satisfactory down to ~260 nm. Below this wavelength, the values determined by Plum et al. considerably differ from both our and NCAR results.

Table 3
Absorption cross sections (cm^2 per molecule) of glyoxal at 295 K (averaged over 1 nm intervals)

λ (nm)	$10^{20}\sigma$	λ (nm)	$10^{20}\sigma$	λ (nm)	$10^{20}\sigma$	λ (nm)	$10^{20}\sigma$	λ (nm)	$10^{20}\sigma$
211	1.310	266	2.050	321	1.810	376	1.260	431	6.350
212	1.170	267	2.080	322	1.650	377	1.310	432	5.490
213	1.050	268	2.130	323	1.610	378	1.490	433	5.330
214	0.942	269	2.180	324	1.600	379	1.430	434	6.230
215	0.850	270	2.240	325	1.530	380	1.850	435	7.190
216	0.792	271	2.340	326	1.550	381	2.340	436	12.100
217	0.725	272	2.450	327	1.610	382	1.820	437	7.610
218	0.664	273	2.560	328	1.840	383	1.850	438	14.500
219	0.618	274	2.670	329	1.760	384	1.790	439	10.500
220	0.581	275	2.750	330	1.560	385	1.780	440	27.700
221	0.546	276	2.810	331	1.040	386	1.790	441	11.500
222	0.507	277	2.850	332	0.989	387	2.160	442	8.870
223	0.505	278	2.870	333	0.939	388	2.880	443	10.400
224	0.493	279	2.890	334	0.853	389	2.970	444	12.400
225	0.492	280	2.920	335	0.677	390	3.360	445	14.900
226	0.474	281	2.990	336	0.597	391	3.910	446	6.950
227	0.466	282	3.100	337	0.563	392	3.860	447	3.550
228	0.472	283	3.210	338	0.639	393	2.760	448	3.850
229	0.464	284	3.330	339	0.550	394	3.030	449	5.280
230	0.489	285	3.450	340	0.518	395	3.780	450	8.200
231	0.504	286	3.570	341	0.555	396	3.430	451	13.300
232	0.522	287	3.610	342	0.480	397	3.220	452	14.600
233	0.529	288	3.620	343	0.469	398	4.170	453	31.100
234	0.535	289	3.620	344	0.651	399	4.020	454	23.600
235	0.554	290	3.560	345	0.602	400	3.710	455	47.200
236	0.580	291	3.470	346	0.710	401	4.320	456	13.500
237	0.623	292	3.470	347	0.600	402	5.730	457	2.620
238	0.658	293	3.510	348	0.506	403	7.030	458	2.100
239	0.683	294	3.550	349	0.390	404	5.930	459	0.884
240	0.719	295	3.620	350	0.366	405	4.300	460	1.110
241	0.741	296	3.660	351	0.374	406	4.170	461	0.972
242	0.760	297	3.760	352	0.417	407	3.870	462	0.693
243	0.796	298	3.890	353	0.390	408	3.090	463	0.326
244	0.845	299	3.960	354	0.378	409	3.870	464	0.351
245	0.906	300	3.900	355	0.414	410	5.560	465	0.454
246	0.963	301	3.740	356	0.409	411	6.740	466	0.497
247	1.000	302	3.610	357	0.415	412	6.500	467	0.236
248	1.040	303	3.430	358	0.447	413	11.000	468	0.066
249	1.060	304	3.220	359	0.470	414	9.890	469	0.045
250	1.090	305	3.120	360	0.539	415	10.300	470	0.033
251	1.140	306	3.120	361	0.555	416	5.640	471	0.040
252	1.200	307	3.070	362	0.603	417	6.580	472	0.056
253	1.280	308	3.020	363	0.551	418	7.640	473	0.059
254	1.350	309	2.990	364	0.584	419	8.840	474	0.072
255	1.420	310	2.960	365	0.580	420	5.060	475	0.116
256	1.460	311	3.100	366	0.647	421	7.170	476	0.119
257	1.490	312	3.220	367	0.766	422	6.950	477	0.243
258	1.520	313	3.250	368	0.927	423	11.500	478	0.122
259	1.550	314	3.080	369	0.954	424	8.050	479	0.036
260	1.610	315	2.570	370	0.997	425	9.670	480	0.018
261	1.690	316	2.520	371	1.070	426	15.500		
262	1.780	317	2.340	372	1.000	427	15.100		
263	1.880	318	2.070	373	1.100	428	21.300		
264	1.950	319	1.820	374	1.230	429	6.070		
265	2.010	320	1.780	375	1.200	430	7.070		

Acknowledgements

We wish to thank Drs. Orlando and Tyndall (NCAR) for making their glyoxal absorption data available prior to its publication.

References

[1] G. Helas, Promet 3/4 (1989) 95.
[2] R.W. Talbot, M.O. Andreae, H. Berresheimer, D.J. Jacob, K.M. Beecher, J. Geophys. Res. 95 (1990) 16799.
[3] D.J. Jacob, S.C. Wofsy, Geophys. Res. 93 (1988) 1477.
[4] K.R. Darnall, R. Atkinson, J.N. Pitts Jr., J. Phys. Chem. 83 (1979) 1943.
[5] R. Atkinson, W.P.L. Carter, K.R. Darnall, A.M. Winer, J.N. Pitts Jr., Int. J. Chem. Kinet. 12 (1980) 779.
[6] J.P. Kilus, G.Z. Whitten, Atmos. Environ. 16 (1982) 1973.
[7] C.N. Plum, E. Sanhueza, R. Atkinson, W.P.L. Carter, J.N. Pitts Jr., Environ. Sci. Technol. 17 (1983) 479.
[8] D. Grosjean, Atmos. Environ. 17 (1983) 2379.
[9] S. Yamamoto, R.A. Back, Can. J. Chem. 63 (1985) 549.
[10] J. G. Calvert, J. N. Pitts Jr., Photochemistry, Wiley, New York, 1966.
[11] R. Atkinson, D.L. Baulch, R.A. Cox, R.F.J.A. Kerr, M.J. Rossi, J. Troe, R. F. Hampson Jr., J. Phys. Chem. Ref. Data (based on data from Ref. [7]) 26 (1997) 521.
[12] J.J. Orlando, G.S. Tyndall, Int. J. Chem. Kinet. 33 (2001) 149.
[13] R. Meller, W. Raber, J.N. Crowley, M.E. Jenkins, G.K. Moortgat, J. Photochem. Photobiol. A: Chem. 62 (1991) 163.
[14] R. Meller, G.K. Moortgat, J. Photochem. Photobiol. A: Chem. 108 (1997) 105.
[15] M.G.M. Berges, P. Warneck, Ber. Bunsenges. Phys. Chem. 96 (1992) 413.
[16] L. Zhu, D. Kellis, C.-F. Ding, Chem. Phys. Lett. 257 (1996) 487.